A Flexible, Stretchable and Shape-Adaptive Approach for Versatile Energy Conversion and Self-Powered Biomedical Monitoring

Po-Kang Yang, Long Lin, Fang Yi, Xiuhan Li, Ken C. Pradel, Yunlong Zi, Chih-I Wu, Jr-Hau He, Yue Zhang, and Zhong Lin Wang**

Flexible and stretchable electronics have attracted long-lasting attentions for their promising applications in next-generation functional devices, including flexible circuitries,[1] stretchable displays,[2] stretchable sensors,[3] epidermal electronics,[4] and implantable devices.[5] This new class of electronics allows devices to be deformed into complex shapes while maintaining the device performance and reliability. However, a sustainable power source is highly desired to drive those electronic devices, and the implementation of traditional power supply remains a challenge due to inconvenient operations and indispensable wire connections. In this regard, a more efficient way is to integrate a power generator to scavenge the ambient energy, especially for the mechanical energy from stretching motions. Attempts have been made to develop flexible and stretchable power generators,[6,7] but their output performances still need further enhancement for practical applications. Recently, triboelectric nanogenerators (TENGs) have been invented based on triboelectrification and electrostatic induction,[8–10] which are demonstrated to be a cost-effective and high-efficient approach for harvesting ambient mechanical energy.[11] Various working modes were developed to accommodate energy conversion from different types of mechanical motions, and high-output power was successfully demonstrated,[12] with numerous applications such as self-powered electronics[13,14] and active sensors.[15]

In this work, we developed a new type of flexible TENG (FTENG), which was fabricated by assembling serpentine-patterned electrodes and a wavy-structured Kapton film. Owing to the unique structural design, the FTENG could be operated at both compressive and stretching mode. At the traditional compressive mode, a high-output power density of 5 W m^{-2} was delivered at a load resistance of 44 MΩ. At the stretching mode, the FTENG was capable of withstanding a tensile strain of up to 22% and its output performance was up to 70 times larger than that of the planar TENG in the control experiment. Moreover, the FTENG was able to provide reliable output performance on curved surfaces (with curvatures of up to 36 cm^{-1}). On the basis of this superior feature, the FTENG could be conformably attached onto human skin for monitoring the gentle motions of joints, muscles, or even the Adam's apple. This research presents an unprecedented advancement in energy harvesting and self-powered sensors, and paves the way for the next-generation stretchable electronics and bio-integrated systems.

The device structure and fabrication process flow of the FTENGs are schematically illustrated in **Figure 1**a. The FTENG is composed of a wavy-structured Kapton thin film sandwiched by two layers of serpentine copper electrodes deposited on stretchable polydimethylsiloxane (PDMS) substrates. First, the super high stretchability of the PDMS substrates was achieved by mixing the elastomer base and curing agent at a 30:1 ratio,[16] by which an optimized stability of the deposited electrode was demonstrated (Figure S1a, Supporting Information). Then, serpentine copper electrodes were deposited on the PDMS membranes by a two-step sputtering approach (see Experimental Section for details). It has been well recognized that the serpentine patterns can provide extraordinary stability to metal electrodes even under tensile strain.[17–20] In this work, the unique advantage of the serpentine electrode was successfully verified by a controlled experiment, in which the conductivities of both linear and serpentine electrodes were monitored upon a series of tensile strains, and the resistance of the serpentine electrode was much lower and more stable than that of the linear electrode, especially under high tensile strains. Finally, a wavy-structured Kapton film was fabricated by a high-temperature annealing process (Experimental Section) and inserted between the two layers of electrodes. It can serve as both the triboelectric material and the spacer layer based on its reversible elastic deformation upon compressing or stretching. Nanowire structures were introduced on both surfaces of the wavy-structured

P. K. Yang, L. Lin, F. Yi, Dr. X. Li, K. C. Pradel, Dr. Y. Zi, Prof. Z. L. Wang
School of Materials Science and Engineering
Georgia Institute of Technology
Atlanta, GA 30332–0245, USA
E-mail: zlwang@gatech.edu

P. K. Yang, Prof. C. I. Wu
Institute of Photonics and Optoelectronics &
Department of Electrical Engineering
National Taiwan University
Taipei 10617, Taiwan, ROC

P. K. Yang, Prof. J. H. He
Computer, Electrical and Mathematical Sciences and Engineering (CEMSE) Division
King Abdullah University of Science & Technology (KAUST)
Thuwal 23955–6900, Saudi Arabia
E-mail: jrhau.he@kaust.edu.sa

F. Yi, Prof. Y. Zhang
State Key Laboratory for Advanced Metals and Materials
School of Materials Science and Engineering
University of Science and Technology Beijing
Beijing 100083, China

Prof. Z. L. Wang
Beijing Institute of Nanoenergy and Nanosystems
Chinese Academy of Sciences
Beijing, China

DOI: 10.1002/adma.201500652

ADVANCED MATERIALS
www.advmat.de

www.MaterialsViews.com

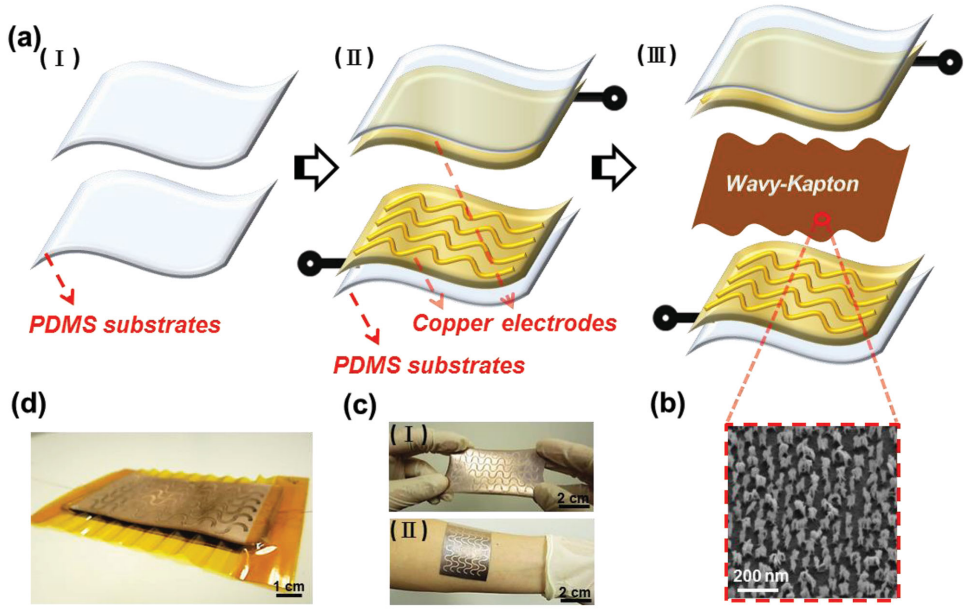

Figure 1. Structure and photographs of the FTENGs. a) Schematic fabrication process flow and device structure of the wavy-FTENG. b) SEM image of nanowire structures on the surface of the Kapton thin film. c) Photographs of the serpentine-patterned electrodes on human skin and under stretching condition. d) Photograph of the fully assembled wavy-FTENG.

Kapton film by the inductively coupled plasmon (ICP) etching process to enhance the triboelectric effect and the effective contact area with the electrodes, as shown in the scanning electron microscopy (SEM) images in Figure 1b and Figure S2 (Supporting Information). The photographs in Figure 1c,d show the morphology of the serpentine electrode and the wavy-structured Kapton film, respectively. It was clearly observed that the FTENG could be conformably attached onto human skin, and the spacing of the FTENG was attributed to the wavy-structured Kapton film. The device area of the obtained FTENG is approximate 40 cm^2, with 7.5 cm in length and 5 cm in width.

Figure 2 illustrates the working principles of the FTENG, which is based on the parallel integration of two single-electrode TENGs[21] with synchronized operations. Owing to the unique structural design, the FTENG is capable of working at both the compressive mode (Figure 2a) and the stretching mode (Figure 2b). As shown in Figure 2a, at the initial state, top and bottom electrodes are separated owing to the stiffness of the wavy-structured Kapton thin film and there is no electric output (I). By applying a vertical compressive force on the FTENG, the copper electrodes and the Kapton thin film are brought into fully contact, leading to contact electrification[22,23] between the electrode surface and the Kapton surface (II). Due to their different surface affinities, the electrons will be transferred from the surface of the electrodes to the surface of Kapton, leaving net negative charges on the Kapton surface and net positive charges on the electrode surface. As the compressive force is releasing, the tribo-charged surfaces get separated owing to the elastic resilience of the wavy-structured Kapton film. The separation of charges will induce potential difference between both electrodes and the ground in the open-circuit condition, which will drive the electrons flowing from the ground to the electrodes in the short-circuit condition. When the compressive force is fully released and the device recovers to its original shape (IV), the open-circuit potential difference will reach its maximum value, since the largest distance between the tribo-charged layers is achieved. Once the FTENG is pressed again (V), the potential difference will start to drop in the open-circuit condition, and the electrons will flow back to the ground in the short-circuit condition until it reaches the fully contact condition (II). Hence, with a periodic compressive force applied onto the FTENG, a cyclic AC output current will be generated across the load between the electrodes and the ground. In conventional designs of the TENGs with vertical contact-separation working mode,[9] an additional spacer was usually indispensable for the charge separation process, while the wave-structured Kapton thin film can serve as both the triboelectric layer for charge generation and the spacer for charge separation, which greatly simplifies the device structure and improves its flexibility.

In the stretching mode, the working principle is quite similar to that of the compressive mode, despite that the direction of the applied force is aligned with the parallel direction of the FTENG. The FTENG is first stretched to the maximum length, and the wavy-structured Kapton thin film will be elongated to flat structure and gets into fully contact with the two electrode layers. Similarly, positive and negative charges will be generated on the surface of the electrode and the Kapton film, respectively, due to the contact electrification between them (II). In the next three steps, the stretching force is first released and then applied again, which will lead to the shrinkage and elongation of the device back and forth. Under the circumstances, the separation distance between the electrode layers and the Kapton film changes in the same manner as that in Figure 2a, which will introduce a similarly cyclic process of the open-circuit potential difference and short-circuit charge transfer between the electrodes and the ground (III to V).

The typical output performance of the FTENG was first investigated on the compressive mode, as shown in **Figure 3**. To demonstrate the significance of the wavy-structured Kapton

DOI: 10.1002/adma.201500652

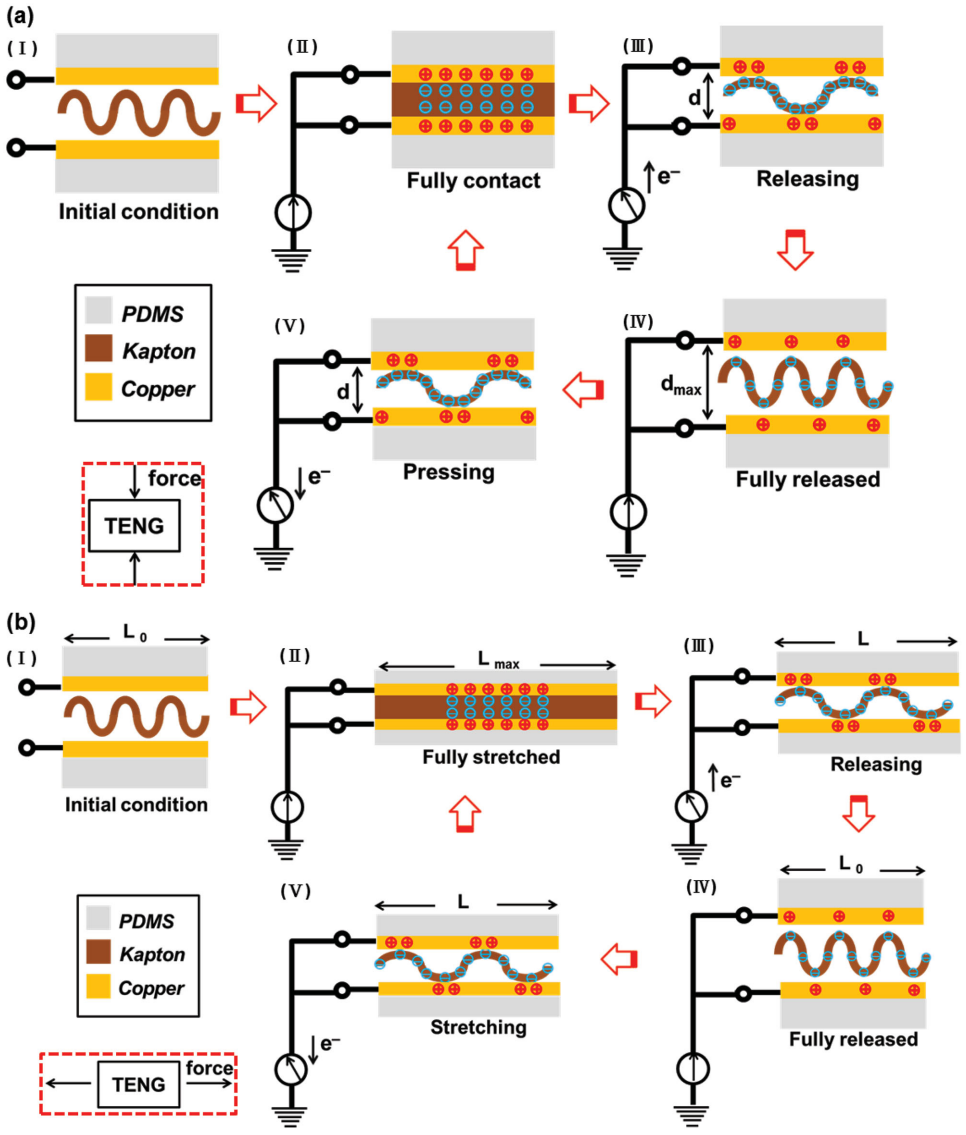

Figure 2. Working principles of the wavy-FTENG. a) Cross-sectional schematics illustrating the power generation process of the wavy-FTENG under a cyclic compressive force. I) Initial state with no force applied; II) A compressive force has been fully loaded onto the FTENG to bring the wavy-structured Kapton thin film and copper electrodes into complete contact; III) The releasing of the compressive force, leading to the separation of the tribo-charged layers; IV) The compressive force has been fully released, with the maximum separation distance between the tribo-charged layers; V) The compressive force is being loaded for the next cycle. The insets show figure legends and the direction of the applied force. b) Cross-sectional schematics illustrating the power generation process of the wavy-FTENG under a cyclic stretching force. I) Initial state with no force applied; II) A stretching force has been fully loaded onto the FTENG to bring the wavy-structured Kapton thin film and copper electrodes into complete stretched condition; III) The releasing of the stretching force, leading to the separation of the tribo-charged layers; IV) The stretching force has been fully released, with the maximum separation distance between the tribo-charged layers; V) The stretching force is being loaded for the next cycle.

film, control measurements were carried out on the TENG with the same materials but a planar Kapton film. In the following discussion, the FTENGs composed of a planar and wavy-structured Kapton films are denoted as the planar-TENG and wavy-FTENG, respectively. Figure 3a–c displays the open-circuit voltage (V_{oc}), the amount of transferred charges (Q_{tr}), and the short-circuit current (I_{sc}) of the planar-TENG and wavy-FTENG. It can be observed that the obtained V_{oc}, Q_{tr}, and I_{sc} are approximate 700 V, 160 nC, and 75 μA for the wavy-FTENG, which are up to 70 times larger than those of the planar-TENG. The significant difference of the output performance could be attributed to the function of the wavy-structured Kapton film as an effective spacer, by which a much larger separation distance is guaranteed. In addition, the triggering frequency is another important factor that can significantly affect the TENG's output.[13] The I_{sc} of the wavy-FTENG under compressive force with different frequencies was measured, as shown in Figure 3d. As the frequency increases from 3 to 10 Hz, the I_{sc} increases from 50 to 85 μA due to the elevation of the deformation rate and thus higher speed of the charge-transfer process.

To evaluate the effective output power of the TENGs, the output current of both the planar-TENG and wavy-FTENG was

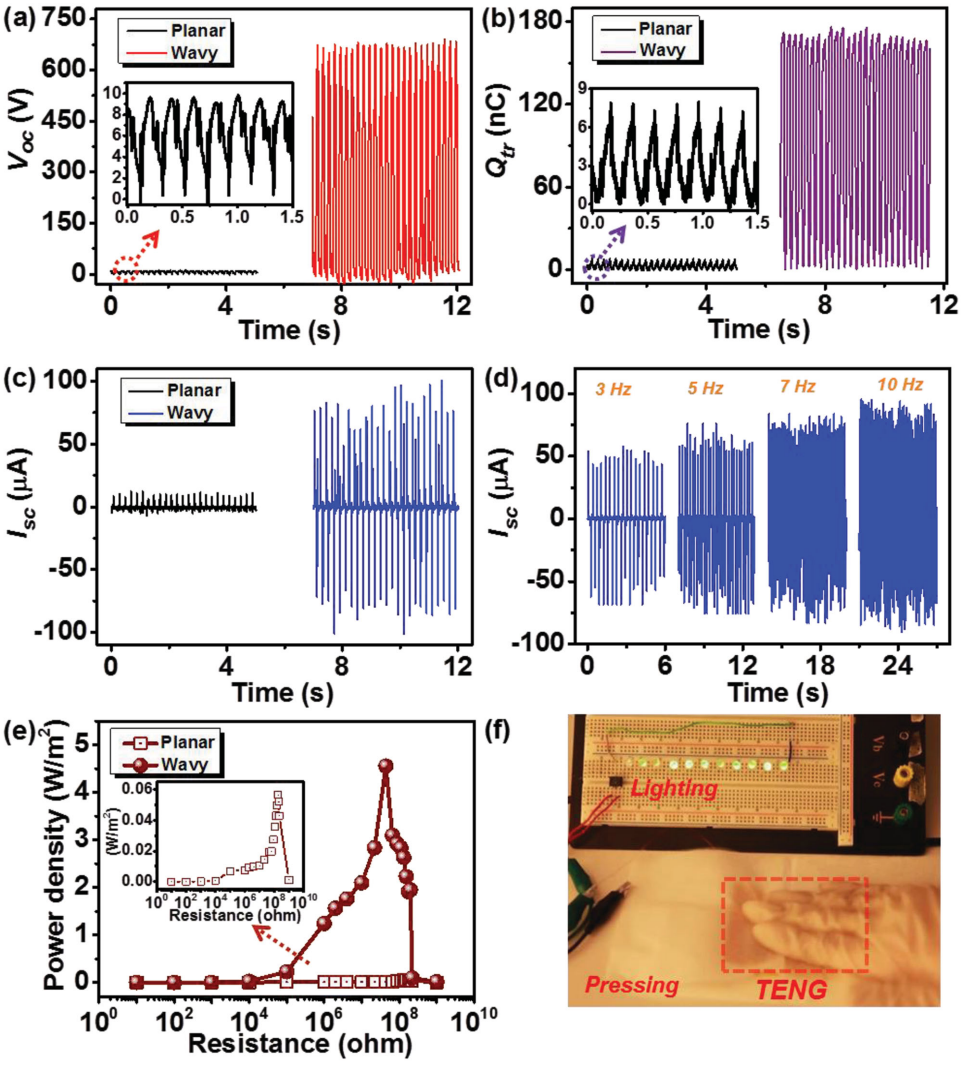

Figure 3. The output performance of the FTENG at compressive mode. a) The open-circuit voltage (V_{oc}) of the planar-TENG and the wavy-FTENG. b) The transferred charge quantity (Q_{tr}) of the planar-TENG and the wavy-FTENG. The inset is an enlarged view of the Q_{tr} in the planar-TENG. c) The short-circuit current (I_{sc}) of the planar-TENG and the wavy-FTENG. The inset is an enlarged view of the I_{sc} of the planar-TENG. d) Frequency responses of the I_{sc} in the wavy-FTENG measured from 3 to 10 Hz. e) Relationship between instantaneous power density and the resistance of the external load for the planar-TENG and the wavy-FTENG. The maximum power density can reach approximate 5 W m^{-2} when the external load is 44 MΩ. f) A photograph showing that 10 commercial green LEDs were directly driven by the wavy-FTENG.

recorded with various resistances in the external load, as shown in Figure S3 (Supporting Information). As expected, the output current of both TENGs was close to the I_{sc} at low-resistance region, but decreased drastically as the resistance kept going up. The effective output power density (P) of the TENGs was calculated as $P = I^2R/A$, where I is the output current across the external load, R is the load resistance, and A is effective size of the TENGs. The relationship between the output power density and the resistance was plotted in Figure 3e, and a high-output power density of 5 W m^{-2} could be achieved for the wavy-FTENG at a load resistance of 44 MΩ, which is much higher than that of the planar-TENG (0.06 W m^{-2} at 176 MΩ). An instantaneous energy conversion efficiency of up to 15% can be achieved at this condition (Figure S4, Supporting Information). Moreover, the relatively smaller optimum resistance of the wavy-FTENG is another advantage in the impedance match for the practical applications of the FTENGs.[24] With such a high-output power, the wavy-FTENG was able to instantaneously power up serially connected light-emitting diodes (LEDs) driven by gentle finger tapping (Figure 3f and Video S1, Supporting Information).

The unique characteristic of the FTENG in this work is to harvest energy from a stretching motion, and the output performance of the FTENG was evaluated by a cyclic stretching force through a linear motor. Again, the performance of the planar-TENG was also measured as a control group. Representative data of the output performance with various tensile strains were recorded for both the planar-TENG and wavy-FTENG in **Figure 4**a–c. It can be found that the V_{oc}, Q_{tr}, and I_{sc} of the wavy-FTENG are monotonically increased with the applied tensile strain of up to 22% (at a maximum operation speed of 0.1 m s^{-1}). The maximum values of the V_{oc}, Q_{tr}, and I_{sc} obtained

Adv. Mater. **2015**,
DOI: 10.1002/adma.201500652

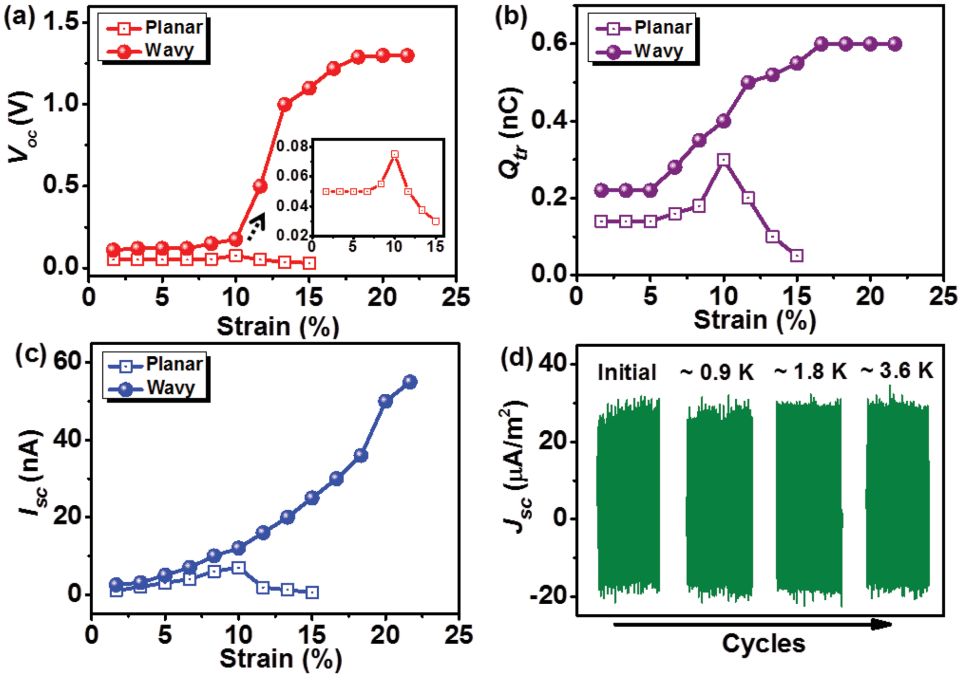

Figure 4. The output performance of the FTENG at stretching mode. a) The V_{oc} of the planar-TENG and wavy-FTENG under various tensile strains. The inset image shows the enlarged view of V_{oc} of the planar-TENG. b,c) The Q_{tr} (b) and the I_{sc} (c) of the planar-TENG and the wavy-FTENG under various tensile strains. d) The measured results of the J_{sc} after the wavy-FTENG has been continuously operated for 900, 1800, and 3600 cycles.

at 22% are 1.3 V, 0.6 nC, and 53 nA, respectively. Conversely, the output performances of the planar-TENG are relatively small and notably decreased after the tensile strain reaches 10%, which can be attributed to the limited spacing between the copper electrodes and planar Kapton thin film. Moreover, after the tensile strain reaches 15%, the largest difference in electric output performance between the planar-TENG and wavy-FTENG can be perceived, with the original data presented in Figure S5 (Supporting Information). From the above-mentioned results, it can be concluded that the wavy-structured kapton film serves as a reliable spacer to maintain the electric output of the FTENG under high tensile strains. Meanwhile, the stability test was carried out by continuously stretching the wavy-FTENG at a speed of 0.1 m s^{-1}, as shown in Figure 4d. After 3600 stretching cycles, the output current density (J_{sc}) exhibits only negligible drops indicating the high durability of the wavy-FTENG.

Another substantial advantage of the wavy-FTENG is its compatibility to work on curved surfaces and adaptability to effectively harvest energy as a bendable power source. To verify this superiority, the output performances of the wavy-FTENG were measured at compressive mode on surfaces with different curvatures (from 12 to 36 cm^{-1}), as displayed in **Figure 5**. As can be observed in Figure 5a–c, the output performances of the wavy-FTENG reveal a great consistency on surfaces with different curvatures, indicating its good versatility to work on non-ideal surface conditions. For example, the wavy-FTENG can be attached on human skin or joints for scavenging energy from human body motions as well as biomedical monitoring, which will be discussed later. On the contrary, the control experiment was conducted by measuring the I_{sc} of the planar-TENG on the surfaces with different curvatures (Figure S6, Supporting Information), and it can be clearly found that the output performance shows an apparent decay with increasing curvatures.

As discussed above, the FTENG could be attached to curved surfaces like human skin as epidermal electronics for both energy harvesting and biomedical monitoring purposes. These potential applications were realized by live demonstrations as shown in **Figure 6** and Videos S2–S6. First, the FTENG was attached onto the joint area of an elbow or knee (Figure 6a,b and Video S2–S3, Supporting Information), and the bending of the joints would lead to the stretching of the device, introducing an output voltage in the measurement. On the other hand, when the FTENG was secured on the bicep of an arm, the tension of the muscle resulted in a compressive force on the FTENG and an output voltage was recorded with distinct polarities (Figure 6c and Video S4, Supporting Information). The FTENG could be utilized for monitoring even more gentle body motions, like the swallowing movements of the human throat (Figure 6d and Video S5, Supporting Information), and a cyclic pulse-like output voltage was recorded in response to the movement of the Adam's apple. Finally, the FTENG was also attached onto the human's neck for detection of the neck movement, as shown in Figure 6e,f and Video S6 (Supporting Information). It could be observed that the tilting direction of the neck could be distinguishable by the polarity of the output voltage, for the FTENG would be compressed when the neck tilted to the left and stretched in the opposite direction. The remarkable sensing capability in monitoring human body motion of the FTENG opens up many potential applications including electronic skins, epidermal electronics, and human–machine interfaces.

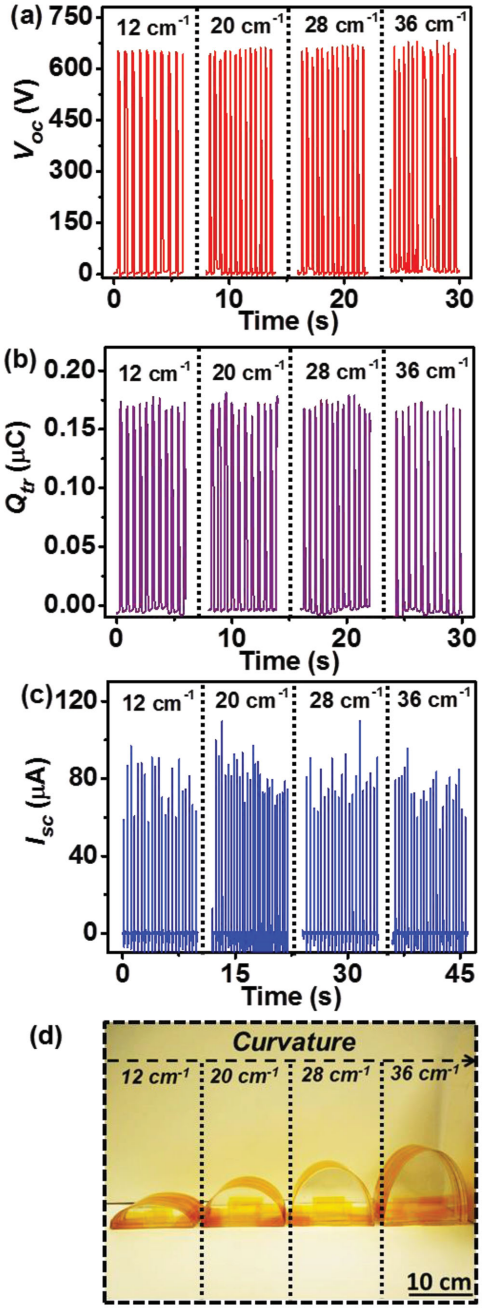

Figure 5. The output performance of the FTENG on curved surfaces. a–c) The V_{oc} (a), the Q_{tr} (b), and the I_{sc} (c) of the wavy-FTENG on the surfaces with different curvatures. d) The corresponding acrylic molds with different curvatures ranged from 12 to 36 cm^{-1}.

In summary, a flexible triboelectric nanogenerator has been developed for energy harvesting from various types of mechanical motions and self-powered body motion sensing. The high stretchability of the FTENG is owing to the advanced structural designs including the wavy-structured Kapton film and the serpentine electrodes on elastic PDMS substrates. The FTENG can be operated at both compressive and stretching mode, and delivers an open-circuit voltage of 700 V and a short-circuit current of 75 μA, corresponding to an instantaneous output power density of 5 W m^{-2}. The wavy-FTENG has presented several advantages as compared to its planar counterpart, such as much higher output performance, the capability of withstanding a tensile strain of up to 22%, and the high stability to work on curved surfaces. Owing to its strong shape adaptability and biocompatibility, the wavy-FTENG could be conveniently attached onto any part of a human body for self-powered body motion sensing, like the detection of joint movement, swallowing, and neck tilting. This work brings up new insights into further development of stretchable TENGs and their biomedical applications, which sheds light on advancements in electronic skins, epidermal electronics, and human–machine interfaces.

Experimental Section

Fabrication of the Serpentine-Patterned Electrode on the PDMS Substrate: The PDMS elastomer and cross-linker (Sylgard 184, Dow Corning) were thoroughly mixed in a 30:1 ratio and degassed for 30 min. Then the fluid mixture was spin-coated (at 100 rpm) onto a PET film (DURALAR) and cured at 85 °C for 1 h in a convection oven. Then, a 200-nm-thick copper electrode was first deposited on the PDMS substrates through a shadow mask with serpentine patterns by magnetron sputtering (PVD75, Kurt J. Lesker). Then, a second sputtering process was conducted to fully cover the PDMS substrates with copper to depress the stickiness of the fresh PDMS surfaces.

The Fabrication of the Wavy-Structured Kapton Thin Film: To create the nanowire structures on the surface of the Kapton thin fim (25 μm), an ICP reactive ion-etching technique was used. Specifically, Ar, O_2, and CF_4 gases were introduced into the ICP chamber with the flow rate of 15.0, 10.0, and 30.0 sccm, respectively. One power source of 400 W was used to generate a large density of plasma, and the other power of 100 W was used to accelerate the plasma ions. The Kapton thin film was etched for 1–5 min, and the length of the as-fabricated nanowire array ranged from 0.4 to 1.1 μm. One power source of 400 W was used to generate a large density of plasma, and the other power of 100 W was used to accelerate the plasma ions. To derive a wavy-structured Kapton thin film, the ICP etched-Kapton thin film was first inserted into a set of stainless rods (with diameter of 1/12 in.). Then the whole set was sent into a muffle oven and cured at 300 °C for 4 h. Since Kapton is a thermoplastic material, the wave shape was maintained permanently after it was cooled down quickly to room temperature.

Assembly of the FTENGs: To assemble the FTENGs, planar Kapton and wavy-structured Kapton thin film were sandwiched between two serpentine-patterned electrodes on PDMS substrates, which correspond to the planar-TENG and wavy-FTENG, respectively. Kapton tapes were used to fix and package the ends of devices, and then copper leads were connected on the electrodes by silver paste for further measurement of electric outputs.

Electrical Measurements of the FTENGs: The surface morphology of Kapton thin film was characterized by LEO 1550 SEM. For the measurement of the electric outputs of the FTENGs, external forces were applied by a commercial linear mechanical motor and a vertical shaker, which correspond to the stretching and compressing operations, respectively. The open-circuit voltage (V_{oc}) and transferred charge (Q_{tr}) were measured by a (Keithley 6514 System) electrometer, while the short-circuit current (I_{sc}) was measured by using an SR570 low-noise current amplifier (Stanford Research System).

Supporting Information

Supporting Information is available from the Wiley Online Library or from the author.

Adv. Mater. **2015**,
DOI: 10.1002/adma.201500652

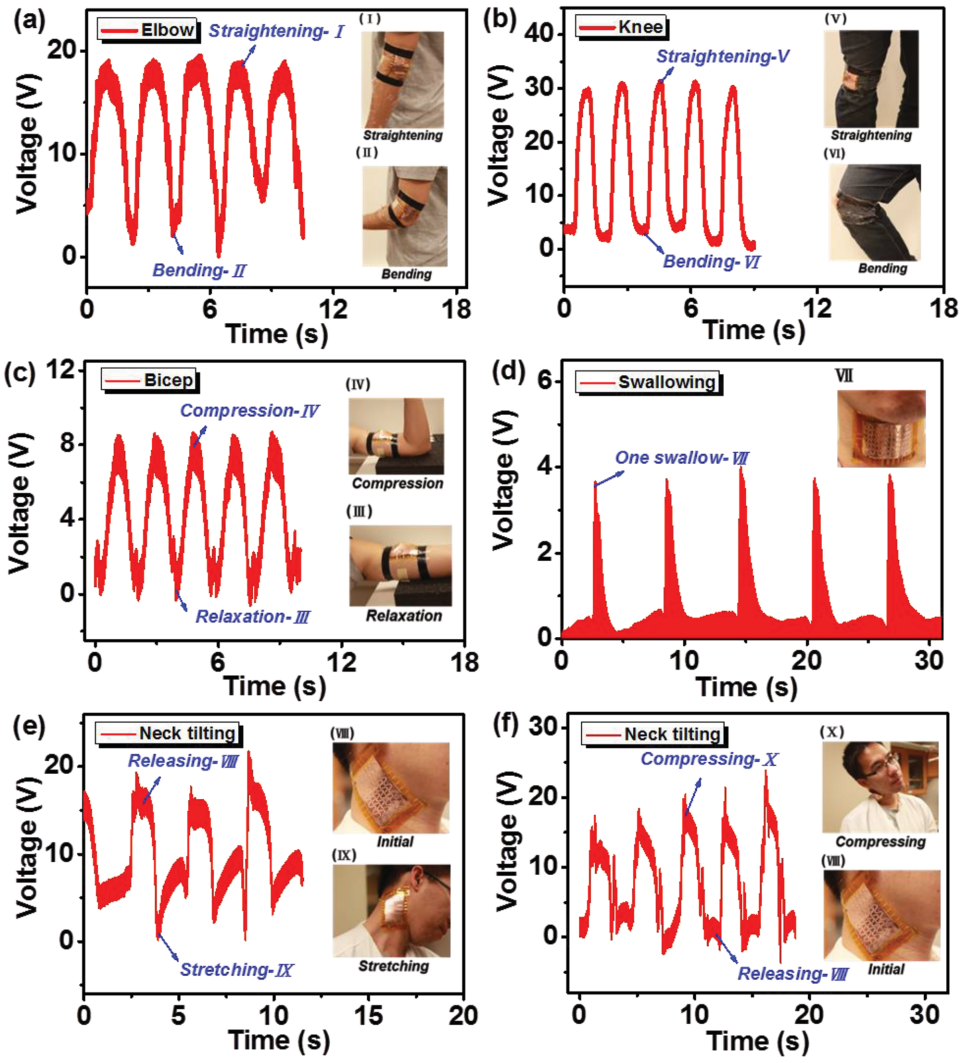

Figure 6. The application of the FTENG for body motion monitoring. Relative changes in voltage versus time for monitoring motions in: a) elbow, b) knee, c) bicep, d) swallowing, e) neck tilting (left), and f) neck tilting (right), respectively. Photographs of the designed sensor adhered to the corresponding parts of the human body are shown as the insets from (I) to (X).

Acknowledgements

P.K.Y. and L.L. contributed equally to this work. Research was supported by Hightower Chair foundation. P.K.Y. thanks the support from the Ministry of science and technology (103–2917-I-002–169), Taiwan.

Received: February 6, 2015
Revised: March 24, 2015
Published online:

[1] D. H. Kim, J. H. Ahn, W. M. Choi, H. S. Kim, T. H. Kim, J. Z. Song, Y. G. Y. Huang, Z. J. Liu, C. Lu, J. A. Rogers, *Science* **2008**, *320*, 507.
[2] T. Sekitani, H. Nakajima, H. Maeda, T. Fukushima, T. Aida, K. Hata, T. Someya, *Nat. Mater.* **2009**, *8*, 494.
[3] T. Yamada, Y. Hayamizu, Y. Yamamoto, Y. Yomogida, A. Izadi-Najafabadi, D. N. Futaba, K. Hata, *Nat. Nanotechnol.* **2011**, *6*, 296.
[4] D. H. Kim, N. S. Lu, R. Ma, Y. S. Kim, R. H. Kim, S. D. Wang, J. Wu, S. M. Won, H. Tao, A. Islam, K. J. Yu, T. I. Kim, R. Chowdhury, M. Ying, L. Z. Xu, M. Li, H. J. Chung, H. Keum, M. McCormick, P. Liu, Y. W. Zhang, F. G. Omenetto, Y. G. Huang, T. Coleman, J. A. Rogers, *Science* **2011**, *333*, 838.
[5] R. H. Kim, D. H. Kim, J. L. Xiao, B. H. Kim, S. I. Park, B. Panilaitis, R. Ghaffari, J. M. Yao, M. Li, Z. J. Liu, V. Malyarchuk, D. G. Kim, A. P. Le, R. G. Nuzzo, D. L. Kaplan, F. G. Omenetto, Y. G. Huang, Z. Kang, J. A. Rogers, *Nat. Mater.* **2010**, *9*, 929.
[6] Y. Qi, J. Kim, T. D. Nguyen, B. Lisko, P. K. Purohit, M. C. McAlpine, *Nano Lett.* **2011**, *11*, 1331.
[7] S. Park, H. Kim, M. Vosgueritchian, S. Cheon, H. Kim, J. H. Koo, T. R. Kim, S. Lee, G. Schwartz, H. Chang, Z. A. Bao, *Adv. Mater.* **2014**, *26*, 7324.
[8] F. R. Fan, Z. Q. Tian, Z. L. Wang, *Nano Energy* **2012**, *1*, 328.
[9] G. Zhu, C. F. Pan, W. X. Guo, C. Y. Chen, Y. S. Zhou, R. M. Yu, Z. L. Wang, *Nano Lett.* **2012**, *12*, 4960.
[10] Z. L. Wang, *ACS Nano* **2013**, *7*, 9533.
[11] Y. N. Xie, S. H. Wang, S. M. Niu, L. Lin, Q. S. Jing, J. Yang, Z. Y. Wu, Z. L. Wang, *Adv. Mater.* **2014**, *26*, 6599.

[12] G. Zhu, J. Chen, T. J. Zhang, Q. S. Jing, Z. L. Wang, *Nat. Commun.* **2014**, *5*, 3426.
[13] S. H. Wang, L. Lin, Z. L. Wang, *Nano Lett.* **2012**, *12*, 6339.
[14] L. Lin, S. Wang, Y. Xie, Q. Jing, S. Niu, Y. Hu, Z. L. Wang, *Nano Lett.* **2013**, *13*, 2916.
[15] L. Lin, Y. N. Xie, S. H. Wang, W. Z. Wu, S. M. Niu, X. N. Wen, Z. L. Wang, *ACS Nano* **2013**, *7*, 8266.
[16] X. Q. Brown, K. Ookawa, J. Y. Wong, *Biomaterials* **2005**, *26*, 3123.
[17] M. Gonzalez, F. Axisa, M. V. Bulcke, D. Brosteaux, B. Vandevelde, J. Vanfleteren, *Microelectron. Reliab.* **2008**, *48*, 825.
[18] Y. G. Sun, W. M. Choi, H. Q. Jiang, Y. G. Y. Huang, J. A. Rogers, *Nat. Nanotechnol.* **2006**, *1*, 201.
[19] S. P. Lacour, J. Jones, S. Wagner, T. Li, Z. G. Suo, *Proc. IEEE* **2005**, *93*, 1459.
[20] D. Y. Khang, H. Q. Jiang, Y. Huang, J. A. Rogers, *Science* **2006**, *311*, 208.
[21] Y. Yang, Y. S. Zhou, H. L. Zhang, Y. Liu, S. M. Lee, Z. L. Wang, *Adv. Mater.* **2013**, *25*, 6594.
[22] L. S. McCarty, G. M. Whitesides, *Angew. Chem. Int. Ed.* **2008**, *47*, 2188.
[23] A. F. Diaz, R. M. Felix-Navarro, *J. Electrostatics* **2004**, *62*, 277.
[24] S. M. Niu, S. H. Wang, L. Lin, Y. Liu, Y. S. Zhou, Y. F. Hu, Z. L. Wang, *Energy Environ. Sci.* **2013**, *6*, 3576.

Adv. Mater. **2015**,
DOI: 10.1002/adma.201500652